High-Performance Flexible Graphene Aptasensor for Mercury Detection in Mussels

Ji Hyun An,[†] Seon Joo Park,[†] Oh Seok Kwon,[†,‡] Joonwon Bae,[§] and Jyongsik Jang[†,*]

[†]World Class University (WCU) Program of Chemical Convergence for Energy & Environment (C_2E_2), School of Chemical and Biological Engineering, Seoul National University, Seoul 151-742, Korea, [‡]Department of Chemistry, Massachusetts Institute of Technology, 77 Massachusetts Avenue, Cambridge, Massachusetts 02139, United States, and [§]Department of Applied Chemistry, Dongduk Women's University, Seoul, Republic of Korea 136-714

ABSTRACT Mercury (Hg) is highly toxic but has been widely used for numerous domestic applications, including thermometers and batteries, for decades, which has led to fatal outcomes due to its accumulation in the human body. Although many types of mercury sensors have been developed to protect the users from Hg, few methodologies exist to analyze Hg^{2+} ions in low concentrations in real world samples. Herein, we describe the fabrication and characterization of liquid-ion gated field-effect transistor (FET)-type flexible graphene aptasensor with high sensitivity and selectivity for Hg. The field-induced responses from the graphene aptasensor had excellent sensing performance, and Hg^{2+} ions with very low concentration of 10 pM could be detected, which is 2−3 orders of magnitude more sensitive than previously reported mercury sensors using electrochemical systems. Moreover, the aptasensor showed a highly specific response to Hg^{2+} ions in mixed solutions. The flexible graphene aptasensor showed a very rapid response, providing a signal in less than 1 s when the Hg^{2+} ion concentration was altered. Specificity to Hg^{2+} ions was demonstrated in real world samples (in this case samples derived from mussels). The aptasensor was fabricated by transferring chemical vapor deposition (CVD)-grown graphene onto a transparent flexible substrate, and the structure displayed excellent mechanical durability and flexiblility. This graphene-based aptasensor has potential for detecting Hg exposure in human and in the environment.

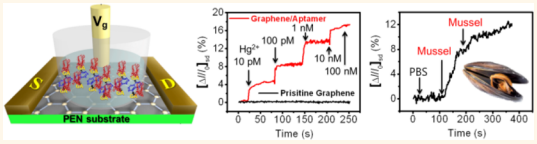

KEYWORDS: graphene · aptasensor · mercury · field-effect transistor · flexible · biosensor

Mercury (Hg) has been used as chemical additive and energy source in industrial development for decades.[1] Hg can be extremely toxic, both to human health and to the environment.[2−4] Hg has been implicated in a number of fatal diseases such as Minamata disease, pulmonary edema, cyanosis and nephrotic syndrome.[5−8] Therefore, the use and manufacture of Hg is regulated in many countries. Hg is still used in many domestic and industrial applications, including thermometers, fluorescent lights, batteries, agricultural chemicals, and cosmetics. To improve safety, various analytical devices have been developed to detect Hg^{2+} ions, including photoelectrochemical methods, colorimetric analysis, and oligonucleotide-based sensors.[9−21] In particular, fluorescence has been widely used owing to the simplicity and high sensitivity. However, fluorescence sensors have limitations including the high cost of the large pieces of equipment, which are not portable.[12−19] Other conventional Hg sensors have significant drawbacks, including a slow time response, low sensitivity and/or poor selectivity. Importantly, the selectivity of these conventional sensors must be improved to discriminate Hg^{2+} ions in real world samples.

Graphene has superb thermally conducting property, excellent mechanical stability, and an extraordinarily high electrical charge carrier mobility. Because of these properties, it has recently become the subject of considerable research interest for a wide range of applications, including supercapacitors, electronic devices, solar cells, transparent conducting electrodes, flexible display devices, biomedical applications and biosensors.[22−28] Graphene has been investigated as a transducer in analytical methodologies, showing high sensitivity, selectivity, and rapid response/recovery times owing to extraordinary carrier mobility and high conductivity.[29] Graphene transferred onto flexible substrates can provide transparent and flexible two-dimensional

* Address correspondence to jsjang@plaza.snu.ac.kr.

Received for review May 29, 2013 and accepted November 26, 2013.

Published online November 26, 2013
10.1021/nn402702w

© 2013 American Chemical Society

thin-sheet, consisting of sp^2-hybridized carbon atoms, with outstanding mechanical properties, leading to the potential for graphene films to be used for wearable and portable biosensor applications. From these attractive advantages, graphene-based flexible substrate is a promising sensing structure for high-performacne flexible biosensors.[30]

Transistor-based sensors, which are the combination of a sensor and amplifier, have potential for the development of miniaturized and portable sensor systems with effective interfacing transfer. Sensors based on graphene transistors have been demonstrated for applications including toxic gas sensors, plasmonic sensors, and optical sensors, displaying excellent sensing performances.[31−33] Graphene transistor can be integrated with liquid-ion gated field-effect transistor (FET) geometry, which can operate in the solution state *via* the gate dielectric. The liquid-ion gated FET system with a graphene transistor has shown excellent stability in the liquid state, as well as low-voltage operation, leading to biosensors for glucose sensors, cell-sensors, DNA sensors, aptasensors, and so forth.[34−37]

Herein, we report a straightforward fabrication methodology for flexible graphene-based aptasensors and demonstrate devices with high sensitivity and selectivity for Hg detection. Chemical vapor deposition (CVD)-grown single-layer graphene was successfully transferred onto a flexible substrate and integrated into the liquid-ion gated FET system *via* surface engineering. The graphene-based aptasensor had a response time of <1 s and a strong field-induced response through the binding between Hg^{2+} ions and the aptamer, leading to a high sensitivity toward Hg^{2+} ions, with a detection limit of 10 pM, which is 2−3 orders of magnitude more sensitive than previously reported Hg sensors based on electrical measurements.[9−11] The FET-type graphene-based Hg sensors displayed high selectivity toward Hg^{2+} ions in mixed solution containing numerous other metal ions and in real world samples derived from mussels. The graphene-based aptasensor was transferred onto a flexible polyethylene naphthalate (PEN) substrate, and the flexible aptasensor system demonstrated excellent mechanical properties. The development of a high-performance flexible FET-type Hg aptasensor based on graphene opens the possibility of Hg detection in the real world.

RESULTS AND DISCUSSION

Fabrication of Flexible Graphene-Based Aptasensor. Figure 1 shows a schematic and design of the flexible graphene-based aptasensor. The single layer graphene was grown on a Cu substrate using chemical vapor deposition (CVD) method, with CH_4 and H_2 gas precursors. The Cu substrate was removed by etching, and the graphene was transferred onto a flexible polyethylene naphthalate (PEN) film. Gold source and drain electrodes were subsequently deposited using thermal evaporation on the graphene-transferred PEN film. The two electrodes were placed side by side and piled up uniform distance. Figure 1a represents a schematic protocol for the fabrication of graphene-based aptasensor on PEN film. The surface of the graphene was chemically modified using 1,5-diaminonaphthalene (DAN), which allowed functionalization using amino groups. The DAN was stacked on the surface of the graphene through $\pi-\pi$ interaction between phenyl groups of the DAN and plane of the graphene.[34] Finally, flexible graphene-based aptasensors were successfully fabricated by the introduction of aptamer after the addition of glutaraldehyde (GA). The DAN and GA were utilized as efficient cross-linking agents for immobilizing the aptamer (3′-amine-TTC TTT CTT CCC CTT GTT TGT-C10 carboxylic acid-5′) on the graphene surface. On the basis of chemical reactions, one aldehyde group of the GA was connected to the amine group of the DAN through chemical bonding by the Schiff-base reaction.[35] Similarly, the other aldehyde group of GA was bound to the amine group at 3′ terminus of the aptamer, resulting in the construction of the stable-sensing elements in the liquid state (Figure 1b). Therefore, the aptamer immobilized on graphene-based aptasensor can specifically interact with Hg^{2+} ions (Figure 1c), leading to the highly sensitive and selective responses.

Characterization of Flexible Graphene-Based Aptasensor. Owing to its outstanding electrical and physical properties, a single layer graphene, rather than double or few layer graphene, has been utilized for various electronic devices such as electrode and electrical transducer of biosensors.[38] The number of layers and thickness of the graphene was characterized using high-resolution transmission electron microscopy (HR-TEM) and Raman analysis. First, an edge of the graphene was observed by HR-TEM, which is an effective method for visually counting the number of layers. Figure 2a shows a HR-TEM image of single layer graphene. Moreover, Raman measurement was also used to analyze the graphene. As shown in Figure 2b, the G peak (~1600 cm^{-1}) and 2D peak (~2700 cm^{-1}) were the most distinctive features of the Raman spectra. In single layer graphene, the 2D peak is sharper and more pronounced than the G peak,[39,40] which is consistent with the spectra shown in Figure 2b, indicating that single layer graphene was successfully fabricated using the CVD method. Figure 2c shows UV−visible spectra of the graphene film at 550 nm; the optical transmittance (Tr) was measured following transfer of the graphene to the flexible PEN substrate and was found to be 97.73%, implying that the thickness of the CVD-grown graphene is similar to general value of a single layer graphene. The inset of Figure 2c shows a photograph of the transparent graphene film. Finally, the thermal stability of flexible graphene film was also maintained, when the gold electrodes deposited on

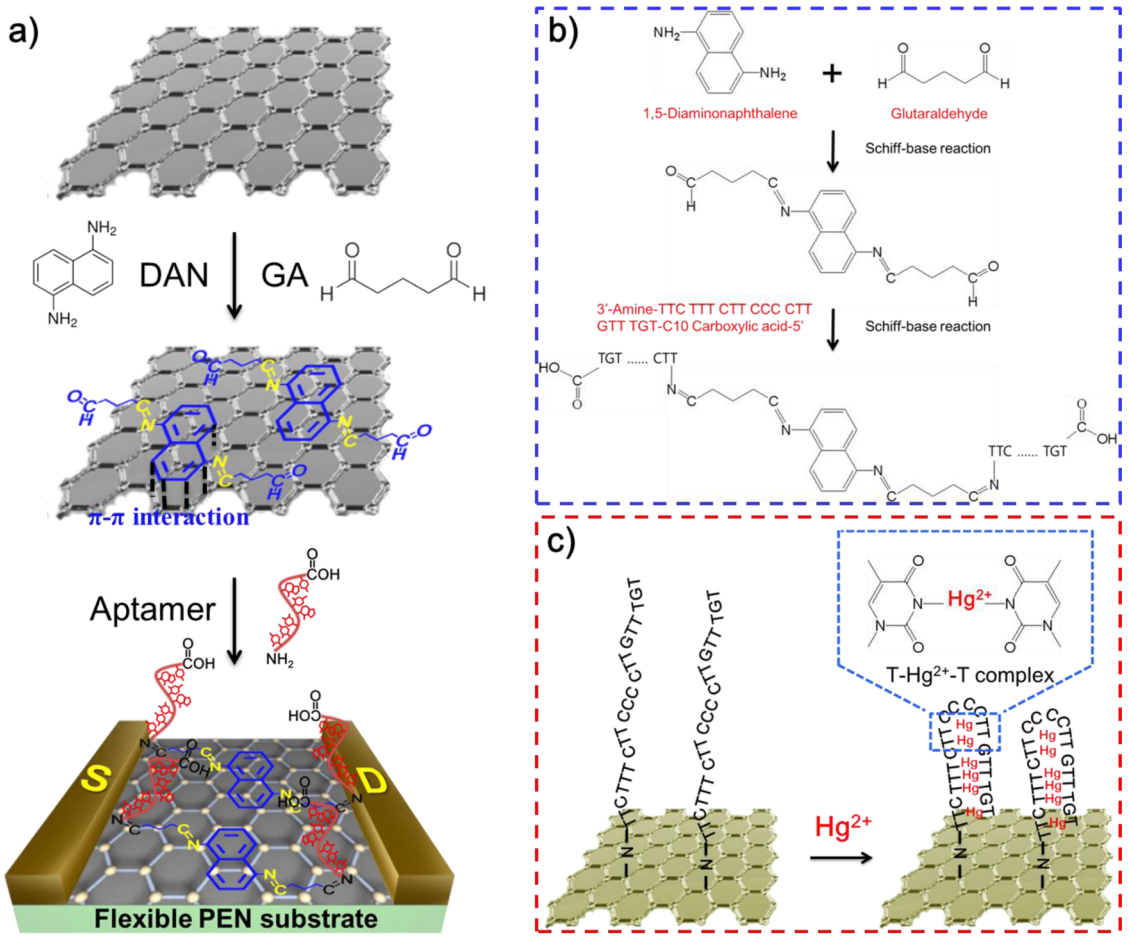

Figure 1. (a) Synthetic protocol of flexible graphene-based aptasensor on PEN film. (b) Chemical reactions among 1,5-diaminonaphthalene (DAN), glutaraldehyde (GA) and the aptamer (3′-amine-TTC TTT CTT CCC CTT GTT TGT-C10 carboxylic acid-5′). (c) Interaction of Hg^{2+} ions with thymine base pairs in the aptamer immobilized on the surface of the modified graphene layer.

the graphene film through thermal evaporation process as shown in Figure 2d.

A field-emission scanning electron microscopy (FE-SEM) measurement was performed to confirm successful immobilization of the aptamer on the surface of the graphene film modified with DAN and GA. Figure 3a,b shows FE-SEM images of the graphene surface before and after the introduction of the aptamer. The graphene film immobilized with the aptamer had a more rough surface (Figure 3b) than the graphene film only, treated with DAN and GA, as shown in Figure 3a. Although significant differences were observed on the surface of the aptamer-immobilized graphene substrate, such as tough surface and band stripes, further characterization was carried out using fluorescence and high-magnification atomic force microscopy (AFM). The fluorescence image of the graphene-based aptasensor shown in Figure 3c clearly shows the aptamers attached on the graphene surface. To observe the fluorescent images, a modified aptamer (3′-amine-TTC TTT CTT CCC CTT GTT TGT-C10 FAM-5′) was prepared.[12] The sequence of the modified aptamer was similar to the aptamer used for Hg detection, except for the functional group at the 5′ terminus. The carboxylic acid group located at the 5′ terminus was substituted with the fluorescein derivative 6-carboxyfluorescein (FAM). Figure 3c shows fluorescence emission between the source and drain electrodes, showing that the aptamer was selectively immobilized on the substrate. Moreover, the aptamer was also observed using high-magnification AFM, as shown in Figure 3d. The vertical value after the introduction of aptamer on the graphene surface using a silicon wafer was measured as *ca.* 3.74 nm by cross-sectional analysis (Figure 3d, inset). The vertical thickness of the aptamer-immobilized graphene significantly increased compared to the heights of single layer graphene as *ca.* 0.9 nm in our previous paper.[37] The concentration of immobilized aptamer on the graphene surface was 1.6 ng/μL (see Supporting Information Figure S1). From these results, the immobilization of aptamer on the graphene surface can be clearly characterized, leading to the stable and strong aptasensor in liquid state.

Electrical Properties of FET-Type Flexible Graphene-Based Aptasensor Geometry. A current−voltage (I−V) analysis was accomplished to the electrical characteristics of

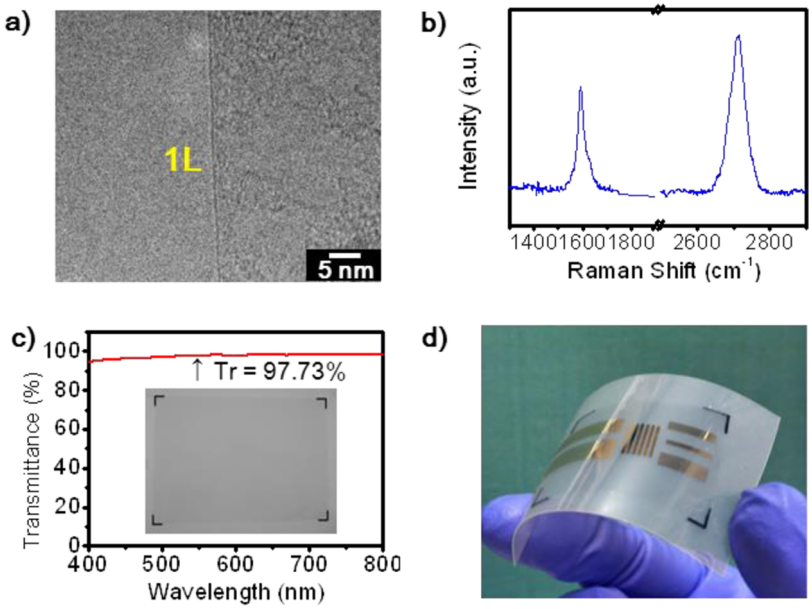

Figure 2. Characterization of single-layer graphene: (a) HR-TEM image and (b) Raman spectra of single layer graphene on a silicon oxide wafer; (c) UV−visible spectra of the graphene transferred on PEN film (transmittance at 550 nm); (d) flexible and transparent graphene film deposited the gold electrodes.

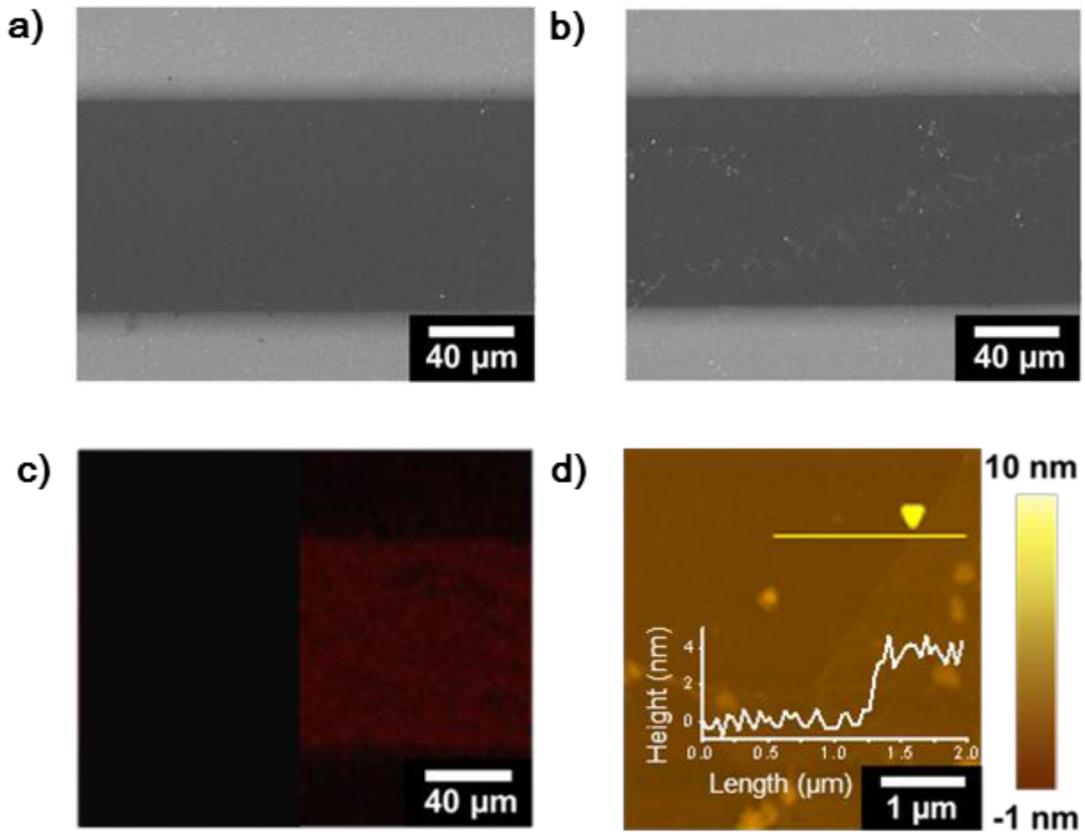

Figure 3. Field-emission scanning electron microscopy (FE-SEM) images of the graphene surface (a) before and (b) after the introduction of the aptamer. (c) Fluorescent image of the modified graphene aptasensor without aptamer (left-side) and with aptamer (right-side). (d) AFM image of the graphene surface immobilized with the aptamer. The yellow line represents a scanning trace of the graphene aptasensor, which is plotted in the inset.

the flexible and transparent aptasensor. Figure 4a represents the dependence of current *versus* voltage before and after the immobilization of the aptamer on the surface of the graphene film. Although d*I*/d*V* value slightly decreased following the attachment of the aptamer, the *I*−*V* relation remained linear, indicating

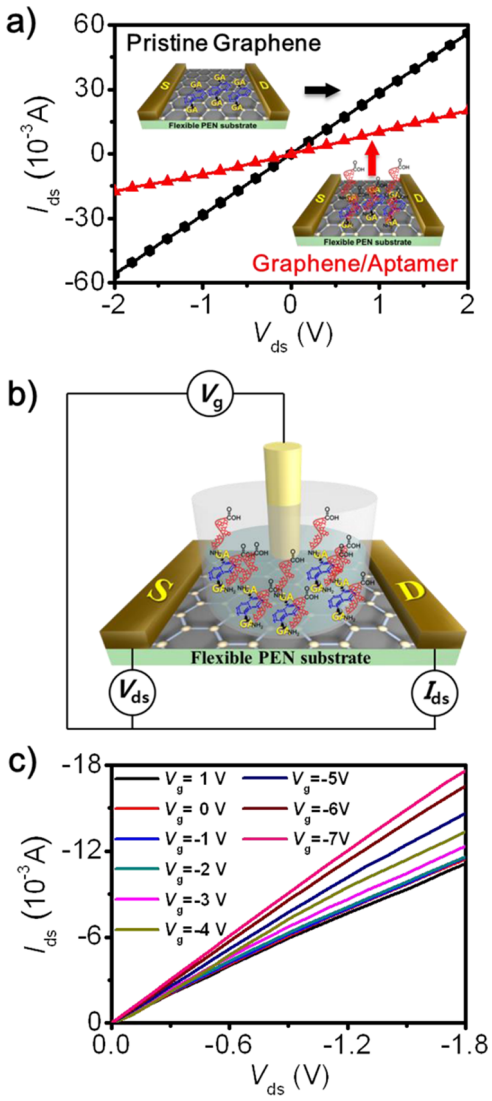

Figure 4. (a) Current−voltage (I−V) curves of the graphene aptasensor before and after the introduction of aptamer. (b) Schematic diagram of a liquid-ion gated FET using graphene conjugated with aptamer. ("V_g", "S" and "D" indicate gating voltage and source/drain electrodes). (c) I_{ds}−V_{ds} output characteristics of the aptasensor at different V_g from 1 to −7 V in a step of −1 V (V_{ds}: 0 to −1.8 V in a step of 50 mV).

that highly stable ohmic contact is preserved after introducing the aptamer. A similar result was observed after the introduction of target ions (see Supporting Information Figure S2). It can be concluded that the conjugation of the aptamer on the graphene surface provided reliable electrical contacts, so that the presence of Hg^{2+} ions as target analyte can be discriminated by monitoring changes in the current that arise due to binding events between the aptamer and the Hg^{2+} ions. Moreover, the introduction of the aptamer on the graphene surface was indirectly observed through changes in the I−V relationship.

To utilize the FET devices as an aptasensor, a liquid-ion gated FET geometry was constructed. The FET geometry was surrounded with a phosphate-buffered solution (PBS; pH 7.4), which helped maintain efficient gate control.[41] Figure 4b shows the experimental setup used to characterize the aptasensor under ambient conditions to investigate changes in the electrical properties in response to the analyte. Figure 4c displays the output characteristics of the aptasensor at different gate voltages (V_g) in a step of −1 V. The drain-to-source current (I_{ds}) negatively increased with negatively increasing gate V_g, providing limited range for p-type (hole-transporting) behavior. Moreover, the ohmic contact characteristics of the I_{ds} curves were maintained for all V_g, demonstrating that electrostatic gating effect of the graphene channel, rather contact resistance, can be the major effect leading to the electrical current changes in the FET device. Judging from these results, the aptamer/Hg^{2+} ion interaction induces a signal of the aptasensor in the liquid phase, leading to the high-performance flexible graphene-based aptasensor.

Real-Time Responses of the FET Type Aptasensor. Graphene is widely known to be an ambipolar material having a Dirac point, which makes the use of graphene in FETs be possible with either p-type or n-type channels.[42] In our previously reported works, sensing devices using graphene also exhibited ambipolar behavior, but had a response that was both more stable and sensitive in the p-type region because of the adsorption of oxygen.[34] Therefore, the real-time responses to the presence of Hg^{2+} ions was characterized as measured at p-type region. The Hg^{2+} ions in solution bind to a specific sequence of the aptamer, and the resulting electrostatic change at the interface, induces a change in the electrical signals. Observing the significant signals allows real-time responses as well as the label-free recognition in the FET device.[43] The sensing performance were confirmed by measuring I_{ds} upon the addition of various mercury concentrations. Figure 5a displays the real-time responses of the aptasensor, as well as that of a pristine graphene substrate for comparison, indicating that the minimum detectable level (MDL) of Hg^{2+} ions was *ca.* 10 pM. Note that this was 2−3 orders of magnitude more sensitive than that of Hg sensors using electrochemical detection. Moreover, the real-time responses from the FET-type graphene-based aptasensor in response to changes in the Hg^{2+} concentration was rapid (on a time scale of less than 1 s) and clearly meaningful (signal-to-noise: 3.2), and also the instantaneous signal changes were observed with wide ranging Hg^{2+} ion concentrations (10 pM to 100 nM). I_{ds} gradually increased when exposed to higher concentrations of Hg^{2+}, and saturated at *ca.* 100 nM, whereas the pristine graphene substrate as a control experiment showed no significant changes in I_{ds}. The increased I_{ds} was observed in current−voltage (I−V) curves of the graphene aptasensor before and after the introduction of Hg^{2+} ions (see Supporting Information Figure S2).

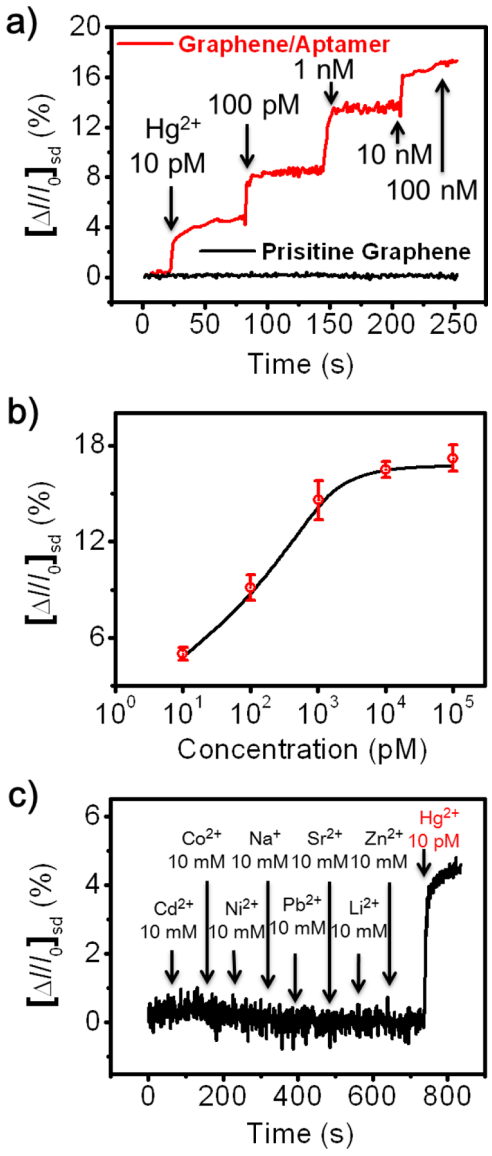

Figure 5. (a) Real-time responses and (b) calibration curve of the aptasensor with various Hg^{2+} concentrations (10 pM to 100 nM). Graphene substrate without aptamer was introduced as a control sample. (c) Selective responses of the aptasensor toward target metal ion (Hg^{2+}, 10 pM) and nontarget metal ions (Cd^{2+}, Co^{2+}, Ni^{2+}, Na^{+}, Pb^{2+}, Sr^{2+}, Li^{2+} and Zn^{2+}, 10 mM).

This is mainly because the specific binding of Hg^{2+} ions is facilitated by the interaction with the thymine base pairs in the aptamer immobilized on the surface of the graphene layer. The Hg^{2+}/thymine interaction proceeds by the displacement of the imino protons of the thymine group with the Hg^{2+} ions, which forms a thymine−Hg^{2+} ion−thymine (T−Hg^{2+}−T) complex. This results in a thermally stabilized duplex structure because the T−Hg^{2+}−T complex is more stable than the adenosine−thymine pair. In other words, the interaction between the thymine base pairs and Hg^{2+} ions is more thermodynamically stable than that of the adenosine−thymine pair. The Hg^{2+} ions immobilized between two thymines can be reduced from the graphene surface, which accumulates holes as majority positive charge carriers forming a p-type FET on the graphene surface. Therefore, adding Hg^{2+} ions at the consistent gate voltage resulted in a positive increase in the drain-to-source current (I_{ds}). This is comparable to a p-type doping effect affecting indirectly on the liquid-ion gate dielectric. The displacement of the imino protons of the thymine group by the positively charged Hg^{2+} ions on the aptamer act as a negative potential gate effect, which increases the hole density in the graphene. Considering these results, specific interactions between the thymine base pairs and Hg^{2+} ions can increase the current of the aptasensor. To further characterize the sensitivity of the response of the graphene-based aptasensor, the change in sensitivity as a function of the Hg^{2+} ion concentration was investigated as shown in Figure 5b. The sensitive change (S) steadily increased from 10 pM to 10 nM of the Hg^{2+} ion concentration. The saturation was observed over 100 nM.

The selective response test toward Hg^{2+} ion was characterized by including 10 mM concentrations of the following nontarget metal ions: Cd^{2+}, Co^{2+}, Ni^{2+}, Na^{+}, Pb^{2+}, Sr^{2+}, Li^{+}, and Zn^{2+}. The results are shown in Figure 5c; when the aptasensor was exposed with nontarget metal ions, no measurable change was observed in I_{ds} (signal-to-noise: <0.168); however, enough large changes in I_{ds} occurred upon addition of 10 pM concentration of Hg^{2+} ions, which is clearly meaningful (signal-to-noise: 3.1327) (see Supporting Information Figure S3). The ability to detect Hg^{2+} ions with a high selectivity was achieved using the aptamer with a sequence that is specific for Hg.

Mercury Discrimination from Real World Sample. To characterize the selectivity of the graphene aptasensor, the mixture with Hg^{2+} ions was dropped into the FET-type geometry. The real-time sensitivity from aptasensor was monitored with significant signal compared to the mixture without Hg^{2+} ions, with the result that the graphene aptasensor can be selective to the Hg^{2+} ions (Figure 6a). On the basis of the result, the real world samples (mussels) were prepared to further confirm the attractive specificity of the aptasensor toward Hg^{2+} ions. Mussels are known as biomonitoring agents of bioavailability and contamination for heavy metals due to their strong metal-binding property, which causes the byssal tissue of the mussel to act as a sensitive biomonitoring organ for heavy metals. Mussels have a stronger interaction with Hg than with other heavy metals through glutathione metabolism in mussel tissues.[44−48] Mussels living in the Sea of Korea were used as real world samples. Inductively Coupled Plasma-Atomic Emission Spectrometer (ICPE) analysis was conducted to measure the concentration of Hg^{2+} ions in the samples; the mussel samples contained a concentration of Hg^{2+} ions from the nature of 0.3749 mM (see Supporting Information Table S1).

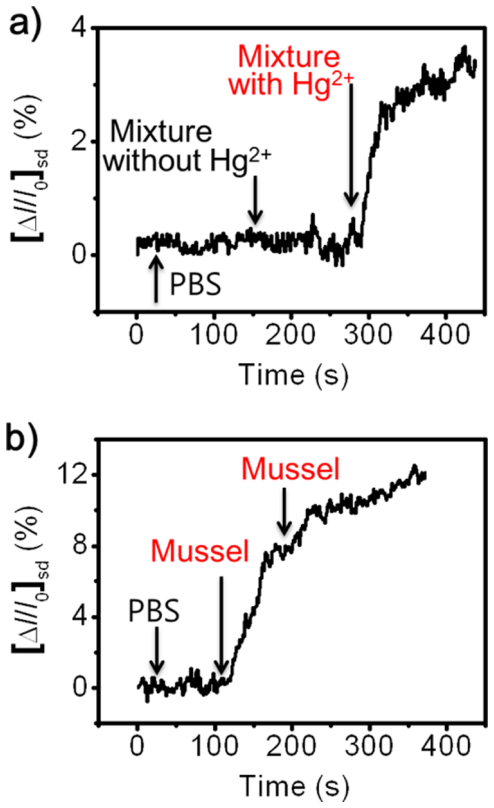

Figure 6. (a) Real-time responses with 10 pM of Hg^{2+} ion in mixture containing 10 mM of the nontarget metal ions. Mixture without Hg^{2+} was used as a control sample. (b) Real-time responses from mussel solution as real world sample.

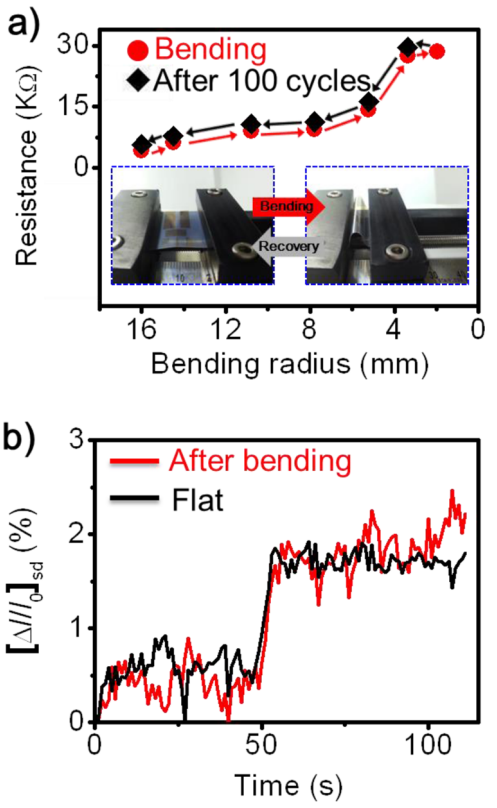

Figure 7. (a) Variation in resistance of a flexible mercury aptasensor based on graphene for different bending radius. (b) Sensing behavior of the aptasensor toward 10 pM of Hg^{2+} after 100 cycles of bending/relaxing.

Figure 6b shows real-time responses of the graphene-based aptasensor to Hg^{2+} ions in the real world samples prepared from the mussels. The current signal change occurred when the aptasensor was exposed to the solution of the mussel sample, demonstrating selectivity toward Hg. As these results show, liquid ion gated FET-type graphene-based aptasensor displays the ability of mercury discrimination in real world samples and it can be applied for extensive real sample applications.

Mechanical Properties of the Graphene Aptasensor. Although many investigations have been carried out to improve the mechanical properties of biological and chemical sensors, fabricating flexible, wearable, and/or portable devices for practical applications remains a challenge. The graphene-based aptasensor on the flexible PEN film has the mechanical flexibility which was investigated by bending structure. Figure 7a indicates bendable resistance of the aptasensor measured with respect to bending radius. The initial resistance before the bending was reconstructed up to a bending radius of *ca.* 2 mm, and also the change of resistance was a small unit even until a bending radius of *ca.* 16 mm. These results suggest that the aptasensor placed on the flexible substrate has a good mechanical stability and resistance. To investigate a sensing ability following mechanical stress, a fatigue test was performed. The graphene-based aptasensor was bent to a radius of *ca.* 2 mm and allowed to relax again, with the process repeated for 100 cycles. Figure 7b displays the sensitive response to 10 pM concentration of Hg^{2+} ions following 100 bending/relaxation cycles; the response decreased by less than 6% following the mechanical stress. As a consequence, the graphene-based aptasensor has extremely good mechanical durability and flexibility, which shows that excellent flexible biosensors can be fabricated.

CONCLUSION

We fabricated a liquid-ion gated FET-type graphene-based aptasensor with highly sensitive and selective responses to various mercury ion concentrations. The aptasensors consisted of a single layer graphene, with the surface of the graphene functionalized using an aptamer that binds specifically to Hg^{2+} ions. The sensing capability of the aptasensor was demonstrated by real-time responses and showed an unprecedented minimum detectable level (10 pM) and rapid response time of <1 s. Moreover, the aptasensor showed outstanding selectivity in mixed solutions containing eight other metal ions. On the basis of the sensing performances of aptasensor, the graphene aptasensor was applied to detect mercury ions in real world

samples, leading to the outstanding mercury selectivity from mussels. In addition, the aptasensor also had excellent mechanical stability and was highly flexible. From these results, liquid-ion gated FET-type graphene-based aptasensor can offer an advanced methodology for state-of-the art mercury analyzing devices and be broadly used for analytical real-sample applications.

MATERIALS AND METHODS

Materials. 1,5-Diaminonapthalene (DAN) and glutaraldehyde (GA) were purchased from Aldrich Chemical Co. Mercury(II) nitrite monohydrate 98% ACS reagent as well as the comparison nontarget materials sodium nitrite, strontium nitrite, lithium nitrite, copper(II) nitrite trihydrate, cadmium nitrite tetrahydrate, cobalt(II) nitrite hexahydrate, nickel(II) nitrite hexahydrate, and zinc nitrite hexahydrate were also purchased from Aldrich. The DNA aptamer for Hg detection was purchased from Bioneer Co. (Daejeon, Korea). The sequence of the aptamer was 3′-amine-TTC TTT CTT CCC CTT GTT TGT-C10 carboxylic acid-5′; the aptamer was modified at the 3′ and 5′ termini. The aptamer stock solution was diluted with TE buffer solution (tris-HCL, EDTA and sterile solution).

Fabrication of Graphene on the Flexible Film. The single layer graphene was fabricated by chemical vapor deposition (CVD) method and it was grown on Cu substrate using CH_4, H_2 gases as carbon source in the cylindrical furnace. The CVD process was as follows: (1) Place the Cu foil in the furnace, evacuate, and introduce 8 ccm flow of H_2 at 90 mTorr for 30 min. (2) Heat to 1000 °C from room temperature, maintaining the elevated temperature for 30 min. (3) Introduce CH_4 at 20 ccm flow and 560 mTorr total pressure for 30 min. (4) Cool the furnace to 200 °C. The Cu substrate was then removed using copper etchant, and the graphene was transferred to the flexible polyethylene naphthalate (PEN) film.

Fabrication of Aptasensor by Surface Modification. To build the FET-type aptasensor into liquid-ion gated device, gold electrodes (W/L = 20; L = 200 μm channel length) were deposited on the graphene film using thermal evaporation. Subsequently, the graphene film with deposited gold electrodes was dipped in 0.02 M DAN with methanol for 15 min. The structure was exposed to 20 μL of 2% GA dissolved in PBS for 2 h, and then the modified graphene film was washed using phosphate-buffered solution (PBS). Finally, the treated graphene film was exposed to 10 nM aptamer (3′-Amine-TTC TTT CTT CCC CTT GTT TGT-C10 Carboxylic acid-5′) for 6 h (40 μL) and then rinsed with PBS.

Instrumentation. All electrical measurements were operated with a Keithley 2612A SourceMeter and probe station (MS TECH, Model 4000). To utilize solution-based measurements, a solution chamber (200 μL volume) was designed and used. The fluorescence microscope (Olympus, model IX2-RFA) was used for monitoring of the atpamer on the surface of modified graphene. The excitation and emission wavelengths of the fluorescence microscope were 488 and 532 μm. To obtain fluorescent images, an AnalySIS TS Auto software was used. The spectrophotometer (Thermo SCIENTIFIC, model NanoDrop 2000/2000c) was used for measuring the concentration of immobilized aptamer on the modified graphene surface. Electrical current change was normalized as $\Delta I/I_0 = (I - I_0)/I_0$, where I_0 is the initial current and I is the detected current for real-time responses.

Conflict of Interest: The authors declare no competing financial interest.

Supporting Information Available: Additional information about the concentration of immobilized aptamer on modified graphene surface, current−voltage ($I-V$) curves of the graphene aptasensor before and after the introduction of Hg^{2+} ions, selective responses of the aptasensor toward target metal ions and Inductively Coupled Plasma-Atomic Emission Spectrometer (ICPE) analysis for mussels. This material is available free of charge *via* the Internet at http://pubs.acs.org.

Acknowledgment. This research was supported by National Research Foundation of Korea (NRF) grant funded by the Korea government (MEST) (No. 2011-0017125).

REFERENCES AND NOTES

1. Fernández, J. A.; Aboal, J. R.; Carballeira, A. Use of Native and Transplanted Mosses as Complementary Techniques for Biomonitoring Mercury around an Industrial Facility. *Sci. Total Environ.* **2000**, *256*, 151–161.
2. Goyer, R. A. Nutrition and Metal Toxicity. *Am. J. Clin. Nutr.* **1995**, *61*, 646S–650S.
3. Nicholson, J. K.; Kendall, M. D.; Osborn, D. Cadmium and Mercury Nephrotoxicity. *Nature* **1983**, *304*, 633–635.
4. Nolan, E. M.; Lippard, S. J. Tools and Tactics for the Optical Detection of Mercuric Ion. *Chem. Rev.* **2008**, *108*, 3443–3480.
5. Clarkson, T. W.; Magos, L.; Myers, G. J. The Toxicology of Mercury—Current Exdposures and Clinical Manifestations. *N. Engl. J. Med.* **2003**, *349*, 1731–1737.
6. Ekino, S.; Susa, M.; Ninomiya, T.; Imamura, K.; Kitamura, T. Minamata Disease Revisited: An Update on the Acute and Chronic Manifestations of Methyl Mercury Poisoning. *J. Neurol. Sci.* **2007**, *262*, 131–144.
7. Geier, D. A.; Geier, M. R. A Case Series of Children with Apparent Mercury Toxic Encephalopathies Manifesting with Clinical Symptoms of Regressive Autistic Disorders. *J. Toxicol. Environ. Health, Part A* **2007**, *70*, 837–851.
8. Korbas, M.; Blechinger, S. R.; Krone, P. H.; Pickering, I. J.; George, G. N. Localizing Organomercury Uptake and Accumulation in Zebrafish Larvae at the Tissue and Cellular Level. *Proc. Natl. Acad. Sci. U.S.A.* **2008**, *105*, 12108–12112.
9. Kim, T. H.; Lee, J.; Hong, S. Highly Selective Environmental Nanosensors Based on Anomalous Response of Carbon Nanotube Conductance to Mercury Ions. *J. Phys. Chem. C* **2009**, *113*, 19393–19396.
10. Chen, K.; Lu, G.; Chang, J.; Mao, S.; Yu, K.; Cui, S.; Chen, J. Hg(II) Ion Detection Using Thermally Reduced Graphene Oxide Decorated with Functionalized Gold Nanoparticles. *Anal. Chem.* **2012**, *84*, 4057–4062.
11. Sudibya, H. G.; He, Q.; Zhang, H.; Chen, P. Electrical Detection of Metal Ions Using Field-Effect Transistors Based on Micropatterned Reduced Graphene Oxide Films. *ACS Nano* **2011**, *5*, 1990–1994.
12. Zhang, L.; Li, T.; Li, B.; Li, J.; Wang, E. Carbon Nanotube-DNA Hybrid Fluorescent Sensor for Sensitive and Selective Detection of Mercury(II) Ion. *Chem. Commun.* **2010**, *46*, 1476–1478.
13. Ono, A.; Togashi, H. Highly Selective Oligonucleotide-Based Sensor for Mercury(II) in Aqueous Solutions. *Angew. Chem., Int. Ed.* **2004**, *43*, 4300–4302.
14. Dave, N.; Chan, M. Y.; Huang, P.-J. J.; Smith, B. D.; Liu, J. Regenerable DNA-Functionalized Hydrogels for Ultrasensitive, Instrument-Free Mercury(II) Detection and Removal in Water. *J. Am. Chem. Soc.* **2010**, *132*, 12668–12673.
15. Guo, C.; Irudayaraj, J. Fluorescent Ag Clusters *via* a Protein-Directed Approach as a Hg(II) Ion Sensor. *Anal. Chem.* **2011**, *83*, 2883–2889.
16. Hollenstein, M.; Hipolito, C.; Lam, C.; Dietrich, D.; Perrin, D. M. A Highly Selective DNAzyme Sensor for Mercuric Ions. *Angew. Chem., Int. Ed.* **2008**, *47*, 4346–4350.
17. Liu, J.; Lu, Y. Rational Design of "Turn-On" Allosteric DNAzyme Catalytic Beacons for Aqueous Mercury Ions with Ultrahigh Sensitivity and Selectivity. *Angew. Chem., Int. Ed.* **2007**, *119*, 7731–7734.
18. Loe-Mie, F.; Marchand, G.; Berthier, J.; Sarrut, N.; Pucheault, M.; Blanchard-Desce, M.; Vinet, F.; Vaultier, M. Towards an Efficient Microsystem for the Real-Time Detection and Quantification of Mercury in Water Based on a Specifically

Designed Fluorogenic Binary Task-Specific Ionic Liquid. *Angew. Chem., Int. Ed.* **2010**, *122*, 434–437.
19. Wegner, S. V.; Okesli, A.; Chen, P.; He, C. Design of an Emission Ratiometric Biosensor from MerR Family Proteins: A Sensitive and Selective Sensor for Hg^{2+}. *J. Am. Chem. Soc.* **2007**, *129*, 3474–3475.
20. Zhang, L.; Chang, H.; Hirata, A.; Wu, H.; Xue, Q.-K.; Chen, M. Nanoporous Gold Based Optical Sensor for Sub-ppt Detection of Mercury Ions. *ACS Nano* **2013**, *7*, 4595–4600.
21. Wen, S.; Zeng, T.; Liu, L.; Zhao, K.; Zhao, Y.; Liu, X.; Wu, H.-C. Highly Sensitive and Selective DNA-Based Detection of Mercury(II) with α-Hemolysin Nanopore. *J. Am. Chem. Soc.* **2011**, *133*, 18312–18317.
22. Bonaccorso, F.; Sun, Z.; Hasan, T.; Ferrari, A. C. Graphene Photonics and Optoelectronics. *Nat. Photonics* **2010**, *4*, 611–622.
23. Lee, Y.-Y.; Tu, K.-H.; Yu, C.-C.; Li, S.-S.; Hwang, J.-Y.; Lin, C.-C.; Chen, K.-H.; Chen, L.-C.; Chen, H.-L.; Chen, C.-W. Top Laminated Graphene Electrode in a Semitransparent Polymer Solar Cell by Simultaneous Thermal Annealing/Releasing Method. *ACS Nano* **2011**, *5*, 6564–6570.
24. Liu, C.; Yu, Z.; Neff, D.; Zhamu, A.; Jang, B. Z. Graphene-Based Supercapacitor with an Ultrahigh Energy Density. *Nano Lett.* **2010**, *10*, 4863–4868.
25. Yoo, J. J.; Balakrishnan, K.; Huang, J.; Meunier, V.; Sumpter, B. G.; Srivastava, A.; Conway, M.; Mohana Reddy, A. L.; Yu, J.; Vajtai, R.; *et al.* Ultrathin Planar Graphene Supercapacitors. *Nano Lett.* **2011**, *11*, 1423–1427.
26. Song, Y.; Wei, W.; Qu, X. Colorimetric Biosensing Using Smart Materials. *Adv. Mater.* **2011**, *23*, 4215–4236.
27. Feng, L.; Wu, L.; Qu, X. New Horizons for Diagnostics and Therapeutic Applications of Graphene and Graphene Oxide. *Adv. Mater.* **2013**, *25*, 168–186.
28. Li, W.; Wang, J.; Ren, J.; Qu, X. Near-Infrared- and pH-Responsive System for Reversible Cell Adhesion Using Graphene/Gold Nanorods Functionalized with i-Motif DNA. *Angew. Chem., Int. Ed.* **2013**, *52*, 6726–6730.
29. Schedin, F.; Geim, A. K.; Morozov, S. V.; Hill, E. W.; Blake, P.; Katsnelson, M. I.; Novoselov, K. S. Detection of Individual Gas Molecules Adsorbed on Graphene. *Nat. Mater.* **2007**, *6*, 652–655.
30. Kuila, T.; Bose, S.; Khanra, P.; Mishra, A. K.; Kim, N. H.; Lee, J. H. Recent Advances in Graphene-Based Biosensors. *Biosens. Bioelectron.* **2011**, *26*, 4637–4648.
31. Song, H. S.; Kwon, O. S.; Lee, S. H.; Park, S. J.; Kim, U.-K.; Jang, J.; Park, T. H. Human Taste Receptor-Functionalized Field Effect Transistor as a Human-like Nanobioelectronic Tongue. *Nano Lett.* **2012**, *13*, 172–178.
32. Fowler, J. D.; Allen, M. J.; Tung, V. C.; Yang, Y.; Kaner, R. B.; Weiller, B. H. Practical Chemical Sensors from Chemically Derived Graphene. *ACS Nano* **2009**, *3*, 301–306.
33. Mohanty, N.; Berry, V. Graphene-Based Single-Bacterium Resolution Biodevice and DNA Transistor: Interfacing Graphene Derivatives with Nanoscale and Microscale Biocomponents. *Nano Lett.* **2008**, *8*, 4469–4476.
34. Park, S. J.; Kwon, O. S.; Lee, S. H.; Song, H. S.; Park, T. H.; Jang, J. Ultrasensitive Flexible Graphene Based Field-Effect Transistor (FET)-Type Bioelectronic Nose. *Nano Lett.* **2012**, *12*, 5082–5090.
35. Kwon, O. S.; Park, S. J.; Hong, J.-Y.; Han, A. R.; Lee, J. S.; Lee, J. S.; Oh, J. H.; Jang, J. Flexible FET-Type VEGF Aptasensor Based on Nitrogen-Doped Graphene Converted from Conducting Polymer. *ACS Nano* **2012**, *6*, 1486–1493.
36. Kwon, O. S.; Ahn, S. R.; Park, S. J.; Song, H. S.; Lee, S. H.; Lee, J. S.; Hong, J.-Y.; Lee, J. S.; You, S. A.; Yoon, H.; *et al.* Ultrasensitive and Selective Recognition of Peptide Hormone Using Close-Packed Arrays of hPTHR-Conjugated Polymer Nanoparticles. *ACS Nano* **2012**, *6*, 5549–5558.
37. Kwon, O. S.; Lee, S. H.; Park, S. J.; An, J. H.; Song, H. S.; Kim, T.; Oh, J. H.; Bae, J.; Yoon, H.; Park, T. H.; *et al.* Large-Scale Graphene Micropattern Nano-biohybrids: High-Performance Transducers for FET-Type Flexible Fluidic HIV Immunoassays. *Adv. Mater.* **2013**, *25*, 4177–4185.
38. Lee, W. H.; Park, J.; Sim, S. H.; Jo, S. B.; Kim, K. S.; Hong, B. H.; Cho, K. Transparent Flexible Organic Transistors Based on Monolayer Graphene Electrodes on Plastic. *Adv. Mater.* **2011**, *23*, 1752–1756.
39. Ferrari, A. C.; Meyer, J. C.; Scardaci, V.; Casiraghi, C.; Lazzeri, M.; Mauri, F.; Piscanec, S.; Jiang, D.; Novoselov, K. S.; Roth, S.; *et al.* Raman Spectrum of Graphene and Graphene Layers. *Phys. Rev. Lett.* **2006**, *97*, 187401.
40. Graf, D.; Molitor, F.; Ensslin, K.; Stampfer, C.; Jungen, A.; Hierold, C.; Wirtz, L. Spatially Resolved Raman Spectroscopy of Single- and Few-Layer Graphene. *Nano Lett.* **2007**, *7*, 238–242.
41. Chen, T.-Y.; Loan, P. T. K.; Hsu, C.-L.; Lee, Y.-H.; Tse-Wei Wang, J.; Wei, K.-H.; Lin, C.-T.; Li, L.-J. Label-Free Detection of DNA Hybridization Using Transistors Based on CVD Grown Graphene. *Biosens. Bioelectron.* **2013**, *41*, 103–109.
42. Yang, X.; Liu, G.; Balandin, A. A.; Mohanram, K. Triple-Mode Single-Transistor Graphene Amplifier and Its Applications. *ACS Nano* **2010**, *4*, 5532–5538.
43. Ohno, Y.; Maehashi, K.; Matsumoto, K. Label-Free Biosensors Based on Aptamer-Modified Graphene Field-Effect Transistors. *J. Am. Chem. Soc.* **2010**, *132*, 18012–18013.
44. Besada, V.; Fumega, J.; Vaamonde, A. Temporal Trends of Cd, Cu, Hg, Pb and Zn in Mussel (Mytilus Galloprovincialis) from the Spanish North-Atlantic Coast 1991−1999. *Sci. Total Environ.* **2002**, *288*, 239–253.
45. Canesi, L.; Viarengo, A.; Leonzio, C.; Filippelli, M.; Gallo, G. Heavy Metals and Glutathione Metabolism in Mussel Tissues. *Aquat. Toxicol.* **1999**, *46*, 67–76.
46. Lee, M.; Rho, J.; Lee, D.-E.; Hong, S.; Choi, S.-J.; Messersmith, P. B.; Lee, H. Water Detoxification by a Substrate-Bound Catecholamine Adsorbent. *ChemPlusChem* **2012**, *77*, 987–990.
47. Struck, B. D.; Pelzer, R.; Ostapczuk, P.; Emons, H.; Mohl, C. Statistical Evaluation of Ecosystem Properties Influencing the Uptake of As, Cd, Co, Cu, Hg, Mn, Ni, Pb and Zn in Seaweed (*Fucus vesiculosus*) and Common Mussel (*Mytilus edulis*). *Sci. Total Environ.* **1997**, *207*, 29–42.
48. Yap, C. K.; Ismail, A.; Edward, F. B.; Tan, S. G.; Siraj, S. S. Use of Different Soft Tissues of *Perna viridis* as Biomonitors of Bioavailability and Contamination by Heavy Metals (Cd, Cu, Fe, Pb, Ni, and Zn) in a Semi-Enclosed Intertidal Water, the Johore Straits. *Toxicol. Environ. Chem.* **2006**, *88*, 683–695.